Title

Probing the Surface of Platinum during the Hydrogen Evolution Reaction in Alkaline Electrolyte

Journal

The Journal of Physical Chemistry B, 122(2)

ISSN

1520-6106

Authors

Stoerzinger, Kelsey A

Favaro, Marco

Ross, Philip N

et al.

Publication Date

2018-01-18

DOI

10.1021/acs.jpcb.7b06953

Peer reviewed

THE JOURNAL OF PHYSICAL CHEMISTRY B

Article

Cite This: J. Phys. Chem. B 2018, 122, 864−870

pubs.acs.org/JPCB

Probing the Surface of Platinum during the Hydrogen Evolution Reaction in Alkaline Electrolyte

Kelsey A. Stoerzinger,[†,$] Marco Favaro,[‡,§,∥,$,&] Philip N. Ross,[⊥] Junko Yano,[§,#] Zhi Liu,[○,▽] Zahid Hussain,[*,‡] and Ethan J. Crumlin[*,‡,%]

[†]Physical and Computational Sciences Directorate, Pacific Northwest National Laboratory, Richland, Washington 99352, United States

[‡]Advanced Light Source, Lawrence Berkeley National Laboratory, 1 Cyclotron Road, Berkeley, California 94720, United States

[§]Joint Center for Artificial Photosynthesis, Lawrence Berkeley National Laboratory, 1 Cyclotron Road, Berkeley, California 94720, United States

[∥]Chemical Sciences Division, Lawrence Berkeley National Laboratory, 1 Cyclotron Road, Berkeley, California 94720, United States

[⊥]Materials Sciences Division, Lawrence Berkeley National Laboratory, 1 Cyclotron Road, Berkeley, California 94720, United States

[#]Molecular Biophysics and Integrated Bioimaging Division, Lawrence Berkeley National Laboratory, 1 Cyclotron Road, Berkeley, California 94720, United States

[○]State Key Laboratory of Functional Materials for Informatics, Shanghai Institute of Microsystem and Information Technology, Chinese Academy of Sciences, Shanghai 200050, People's Republic of China

[▽]Division of Condensed Matter Physics and Photon Science, School of Physical Science and Technology, ShanghaiTech University, Shanghai 200031, China

[%]Joint Center for Energy Storage Research, Lawrence Berkeley National Laboratory, 1 Cyclotron Road, Berkeley, California 94720, United States

Supporting Information

ABSTRACT: Understanding the surface chemistry of electrocatalysts in *operando* can bring insight into the reaction mechanism, and ultimately the design of more efficient materials for sustainable energy storage and conversion. Recent progress in synchrotron based X-ray spectroscopies for in *operando* characterization allows us to probe the solid/liquid interface directly while applying an external potential, applied here to the model system of Pt in alkaline electrolyte for the hydrogen evolution reaction (HER). We employ ambient pressure X-ray photoelectron spectroscopy (AP-XPS) to identify the oxidation and reduction of Pt-oxides and hydroxides on the surface as a function of applied potential, and further assess the potential for hydrogen adsorption and absorption (hydride formation) during and after the HER. This new window into the surface chemistry of Pt in alkaline electrolyte brings insight into the nature of the rate limiting step, the extent of H ad/absorption, and its persistence at more anodic potentials.

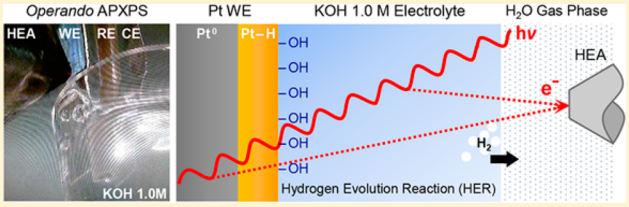

INTRODUCTION

Goals to sustainably store and convert fuel motivate the continued development of electrolyzers and fuel cells to convert between electrical and chemical energy.[1−6] These systems require not only efficient, durable, and cost-effective materials but also the precise design of electrochemical interfaces. Progress can be greatly aided by the availability of *operando* techniques to probe the structure and composition of the dynamic electrified solid/liquid interface.[7−13] Platinum, while scarce and expensive,[14] offers a model system to provide surface chemical and structural transformation insights under various (electro)chemical reaction environments. In depth study of the material aims to expedite the development of Pt alternatives with tailored physical/chemical properties that surpass current state of the art alkaline electrocatalysts.[15−17]

The hydrogen evolution reaction (HER) has been the subject of intense investigation as a critical reaction in electrochemical energy storage.[5,18,19] Pt, a prototypical electrocatalyst highly active for the HER under acidic conditions,[20] is 2 orders of magnitude less active under alkaline conditions.[21] The initial formation of the active adsorbed hydrogen from water is typically considered kinetically difficult under alkaline conditions,[22,23] although the hydrogen binding energy has been used as an activity descriptor for HER on Pt[24] and other metals

Special Issue: Miquel B. Salmeron Festschrift

Received: July 14, 2017
Revised: November 17, 2017
Published: November 22, 2017

DOI: 10.1021/acs.jpcb.7b06953
J. Phys. Chem. B 2018, 122, 864−870

under alkaline conditions as well.[25] pH dependence of the hydrogen binding energy has been proposed to be responsible for the lower activity under alkaline conditions, where the H-binding is stronger.[26,27] Others have suggested that the HER activities can be enhanced in alkaline solution by the inclusion of more oxophilic sites to enhance OH adsorption, such as in $Pt_{0.1}Ru_{0.9}$[28] and Pt−Ni.[16] However, the ubiquitous adsorption of water on the electrode interface and its orientation may also influence the reaction kinetics.[29]

The hydrogen "charge" current can be used to estimate surface area on the basis of the presence of a single monolayer (ML) coverage—one H atom for every Pt[30]—under relatively well-defined conditions of electrochemical potential and sweep rate.[31] However, in some circumstances, H may be absorbed interstitially[32] among the first layer of metal atoms.[33,34] Diffusion of H into the metal could also be possible with extended polarization at cathodic potentials,[35] and the formation of Pt hydride has been discussed for small particles and alloys.[36,37] Probing adsorbed H and the possibility of absorbed H within buried layers is experimentally challenging, yet it could offer great insight into the chemical speciation of Pt in *operando*.

To achieve a molecular-level comprehension of the HER mechanism, we studied a polycrystalline Pt electrode surface under cathodic conditions in an alkaline electrolyte, by means of *operando* APXPS performed with "tender" X-rays ($h\nu$ = 4 keV) directly at the electrified solid/liquid interface.[38,39] We report the surface speciation of Pt and its oxides as a function of applied potential, and find under HER conditions $Pt^{(II)}O$ and $Pt^{(IV)}O_2$ species are reduced. However, a new Pt component at higher binding energies is present in the Pt 4f but not observed in the O 1s spectra. We propose this arises from the formation of Pt−H species, which persist after HER where the open circuit potential is more cathodic from the adsorption of H.[40] Electrochemical cycling to strip adsorbed H reduces protonated species at the binding energy of $Pt^{\delta}-OH_{ads}$, while the persistence of a Pt−H feature suggests this species may exist within Pt subsurface layers.

METHODS

"Dip and Pull" Method and *operando* Measurements. The working electrode (WE), reference electrode (RE), and counter electrode (CE) were mounted into a PEEK electrode housing. Electrical feedthrough within the multiaxis manipulator connected the electrodes to an external potentiostat/galvanostat (Biologic SP 300) to perform *operando* electrochemistry measurements. The WE and the analyzer front cone were commonly grounded.

The 0.1 M KOH aqueous electrolyte was outgassed prior to introduction into the experimental chamber for >30 min at low pressure (∼10 Torr) in a dedicated offline chamber. After placing the manipulator and the outgassed electrolyte into the APXPS experimental chamber, the pressure was carefully lowered down to the water vapor pressure (between 16 and 20 Torr, at room temperature, r.t.).

To create a solid/liquid interface (WE/electrolyte), all three electrodes were immersed into the electrolyte and then slowly extracted from the electrolyte solution by raising the manipulator at a constant vertical rate. This procedure results in a thin layer of liquid electrolyte film remaining on the Pt electrode (typically 10−30 nm) above the bulk electrolyte, moved to the focal point of the analyzer in order to perform an XPS investigation of the solid/liquid interface as a function of the applied potential. During the measurements, the bottom parts of the electrodes were kept in the bulk electrolyte, in order to ensure electrical continuity between the thin electrolyte layer on the WE surface and the bulk electrolyte itself.

Electrochemical Measurements. Milli-Q water (DI, ρ = 18.2 MΩ cm) and potassium hydroxide (KOH, 99.99%, Aldrich) were used as solvent and supporting electrolyte, respectively. A miniaturized leakless $Ag/AgCl/Cl^-_{(sat.)}$ RE (ET072-1, eDAQ) was used (standard electrode potential $E^{\circ}_{Ag/AgCl(sat.)}$ = 197 mV with respect to the normal hydrogen electrode, NHE). All of the potentials reported in this work are referred to this RE. The WE and CE (Pt polycrystalline foils, 99.99%, thickness 0.5 mm, Aldrich) were polished to a mirror finish with silicon carbide papers of decreasing grain size (Struers, grit: 2400 and 4000). The samples were then cleaned by two cycles of ultrasonic treatment in a mixture of Milli-Q water/ethanol (Aldrich, 1:1) for 10 min. A third ultrasonic cleaning was then conducted in pure Milli-Q water for 15 min, followed by a thorough rinsing and drying in N_2 stream.

An electrochemical cleaning procedure was conducted by holding the Pt WE at −1200 mV (within the hydrogen evolution reaction, HER, region) for 30 min, in order to obtain a pure metallic (Figure S1) and a homogeneous surface, increasing in this way the experimental reproducibility. Survey spectra (Figure S2) verify no unexpected elements are present on the Pt electrode or KOH electrolyte. The cleaning procedure was stopped after reaching the current open circuit potential (OCP) of the cell from the cathodic side. The data acquisition started only when the OCP reached a stable value over the observation time (about 30 min). All cyclic voltammetry measurements were conducted at a scan rate of 20 mV s^{-1}. The WE was held potentiostatically under OER (900 mV) and HER (−850 mV) conditions. Electrochemical impedance spectroscopy was performed with a peak-to-peak voltage amplitude of 10 mV (Table S1).

Beamline 9.3.1 and APXPS Experimental Details. Beamline 9.3.1 at Advanced Light Source (ALS, Lawrence Berkeley National Laboratory) is equipped with a bending magnet and a Si(111) double crystal monochromator (DCM) having a total energy range between 2.0 and 7.0 keV ("tender" X-ray range).[38,39,41−43] The minimal spot size at the beamline is 0.7 mm (w) × 1.0 mm (h).

The pass energy of the Scienta analyzer (R4000 HiPP-2) was set to 200 eV, using a step of 100 meV and a dwell time of 300 ms, to give a total resolution (X-rays and analyzer) of ∼250 meV at r.t. and at 4 keV. The measurements were taken using a photon energy of 4 keV at r.t. and in normal emission, at a pressure in the experimental chamber matching the water vapor tension at r.t. (16−18 Torr). The detection stage in the analyzer (multichannel plate) was kept under high vacuum conditions (∼10^{-7} Torr) by a differentially pumped electrostatic lens system. To limit the evaporation from the electrochemical cell, a larger outgassed solution buffer was placed in the analysis chamber.

Spectral fitting (Table S2) was carried out using CasaXPS and employing a Shirley background. A Doniach−Šunjić shape was used for the metallic Pt^0 4f photoelectron peaks, calibrating the binding energy (BE) scale such that the metal component was at 71.2 eV.[41] The use of a line shape with greater asymmetry did not influence the observed trends in surface speciation. The gas phase water (GPW) and liquid phase water (LPW) in the O 1s spectra were fit with a 25:75

DOI: 10.1021/acs.jpcb.7b06953
J. Phys. Chem. B 2018, 122, 864−870

Lorentzian:Gaussian symmetrical Voight function, and all other peaks were fit with a 20:80 Lorentzian:Gaussian ratio. Variation in this ratio for the dominant GPW and LPW peaks did not influence the observed trends in surface speciation. Differential charging, likely from salt on the analyzer cone, required the O 1s BE scale to be separately calibrated from the Pt 4f. The LPW peak for the initial OCP (−200 mV) was fixed to that of ref 41 and in subsequent spectra calibrated to the expected LPW location accounting for a 1:1 increase in BE with reducing potential. Similar to how Kolb measured a change in work function from adsorbed layers,[44] such a correlation between applied potential and electrolyte BE relative to the grounded WE has been reported previously with the dip-and-pull technique.[38,39,41,43]

RESULTS AND DISCUSSION

***Operando* Spectroscopy of the Solid/Liquid Interface.** The surface chemistry of a Pt electrode was studied by APXPS in *operando*—as a function of applied potential at a solid/liquid interface—as shown in Figure 1a. The "dip and pull" procedure[38,39,41−43] enables simultaneous photoelectron spectroscopic characterization of the ∼20 nm 1.0 M KOH aqueous electrolyte and ∼10 nm of the Pt WE[41] while undergoing electrochemical reactions at the electrified solid/liquid interface. The polycrystalline Pt WE and analyzer share a common ground, with potential controlled relative to the Ag/AgCl/$Cl^-_{(sat.)}$ RE and current balanced by the CE in the three-electrode electrochemical cell.

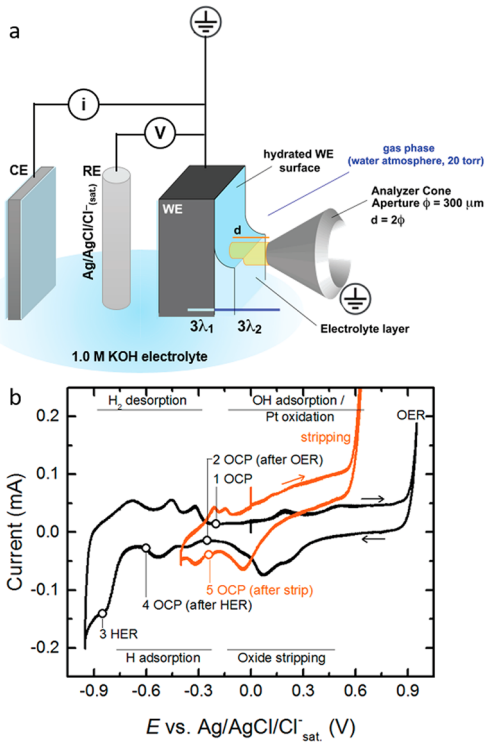

Figure 1. (a) Schematic of the *operando* experimental setup at beamline 9.3.1 at the Advanced Light Source. The manipulator holds the Pt working electrode (WE), reference electrode (RE), and Pt counter electrode (CE). The photoelectron inelastic mean free path in the Pt WE (λ_1) is smaller than that in the liquid−gas atmosphere (λ_2). (b) Cyclic voltammetry (CV) at room temperature and $p \sim 18$ Torr (obtained with a scan rate of 20 mV s^{-1}) with the electrodes immersed, noting the potential ranges for changing surface chemistry, the oxygen evolution reaction (OER), and the hydrogen evolution reaction (HER). The potentials at which APXPS was performed are noted in chronological order: 1, initial open circuit potential (OCP); 2, OCP after OER; 3, HER; 4, OCP after HER; 5, OCP after stripping. The orange CV reflects the so-called "stripping" when the working electrode is polarized to oxidizing conditions after potentiostatic holding under HER conditions.

We performed cyclic voltammetry (CV) measurements (Figure 1b) to study the evolution of the current as a function of applied potential. The current associated with the thin electrolyte film is $\sim^1/_3$ that of the total current.[41] Sweeping to more anodic (positive) potentials, the Pt surface adsorbs hydroxyl species and oxidizes,[45−47] eventually evolving O_2 from soluble hydroxyl species in OER. Reversing the sweep direction results in oxide stripping prior to the return to OCP. Going to more cathodic (negative) potentials, H atoms adsorb on the surface prior to their evolution in HER, and returning to OCP pass through a region of H_2 desorption.[48] After HER polarization, H atoms can be stripped from the surface, and dissolved H_2 oxidized in the hydrogen oxidation reaction.[49]

In order to examine changes in the Pt adsorbates and surface chemistry under these conditions, we held the WE at constant select potentials to perform chronoamperometry while simultaneously characterizing the surface species using APXPS. The following conditions were considered, with the corresponding potentials indicated in Figure 1b: 1, the initial OCP (E = −200 mV); 2, OCP following potential holding at OER conditions (−250 mV); 3, HER (−850 mV); 4, OCP following potential holding at HER conditions (−600 mV); 5, OCP following stripping (−240 mV).

The O 1s spectra exhibit spectral components originating from both the solid and liquid phases (Figure 2a). Species present on the WE remain at constant BE regardless of applied potential, and include oxidized platinum ($Pt^{(II)}O$)[47,50] centered at 530.4 eV, adsorbed hydroxyls ($Pt^{\delta}-OH_{ads}$) at 531.3 eV, and chemisorbed water (H_2O_{chem}) centered at 532.4 eV.[41] Species that remain in the liquid phase shift linearly to higher BE with a more negative applied potential (Figure 2b),[38] including LPW and soluble hydroxyls (OH_{sol}), with similar behavior observed in the GPW. At the initial OCP (−200 mV), some $Pt^{(II)}O$ persists on the surface, and remains after performing OER (−250 mV). Furthermore, under alkaline conditions, hydroxyl species adsorb on activated Pt sites ($Pt^{\delta}-OH_{ads}$),[51−53] observable both before and after OER. Polarizing to cathodic conditions for HER (−850 mV), $Pt^{(II)}O$ species are reduced and no longer present on the surface, and remain negligible upon resting to OCP after HER (−600 mV) and at OCP after stripping (−240 mV). In contrast, $Pt^{\delta}-OH_{ads}$ and H_2O_{chem} remain on the surface at all potentials investigated.

Understanding the Pt Surface in *operando*. We next consider speciation of the Pt WE via the metal 4f core level. The spectra (Figure 3) can be deconvolved into four components known to persist under oxidative conditions,[47,54] noting the BE of the $4f_{7/2}$ level (with a 3.3 eV spin−orbit splitting): Pt^0 metal (71.2 eV), $Pt^{\delta}-OH_{ads}$ (71.8 eV), $Pt^{(II)}O$ (72.5 eV), and $Pt^{(IV)}O_2$ (74.6 eV). Fitting the initial OCP with these constraints yields a composition consistent with that obtained from the O 1s, with both $Pt^{\delta}-OH_{ads}$ and $Pt^{(II)}O$ present with comparable intensities. Comparison of the intensities with the respective components in the O 1s spectra leads to an empirical estimation of the O:Pt relative sensitivity factor (RSF) at the electrode surface, providing quantitative bounds for the $Pt^{\delta}-OH_{ads}$ and $Pt^{(II)}O$ in the Pt 4f by fitting of

DOI: 10.1021/acs.jpcb.7b06953
J. Phys. Chem. B 2018, 122, 864−870

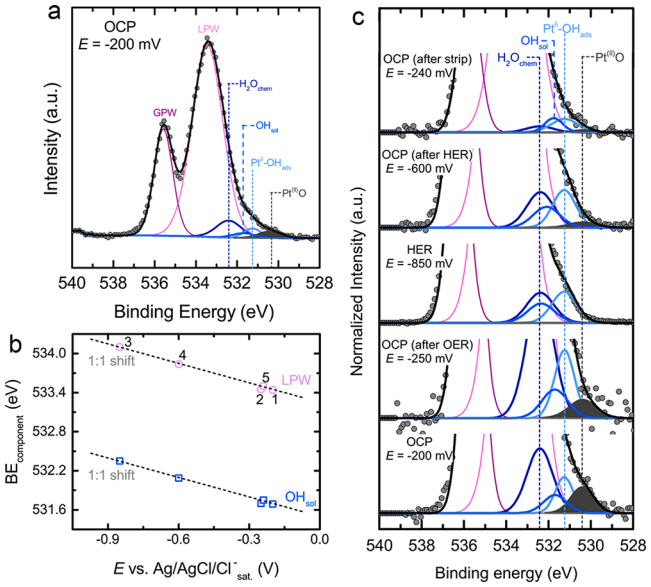

Figure 2. (a) *Operando* APXPS O 1s photoelectron peak at 4 keV at OCP. The gas phase water (GPW), liquid phase water (LPW), chemisorbed water (H_2O_{chem}), soluble hydroxyls (OH_{sol}), adsorbed hydroxyls (Pt^{δ}–OH_{ads}), and oxidized platinum ($Pt^{(II)}O$) features are noted. (b) The BE of solution species LPW and OH_{sol} shift 1:1 with applied potential, while species on the surface remain fixed. (c) Magnification of the O 1s, background subtracted and normalized to the intensity of the Pt^0, as a function of applied potential, illustrating the changing surface species. The full spectrum for the HER condition is presented in Figure S3.

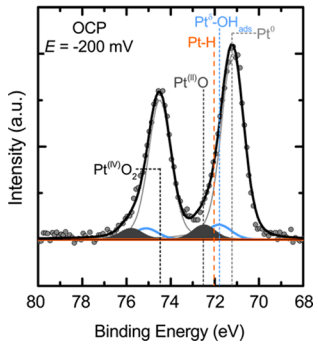

Figure 3. *Operando* APXPS Pt 4f photoelectron peak at 4 keV for the starting OCP condition. Indicated is the position of the Pt^0 metal, Pt^{δ}–OH_{ads}, Pt–H, $Pt^{(II)}O$, and $Pt^{(IV)}O_2$ peaks.

the O 1s spectra (Figure 4). With this constraint on the intensity of oxygenated Pt species, we observe the intensity at ~72.1 eV is underfit at reducing potentials (Figure S4). To account for that, a new spectral component of unconstrained BE and intensity is added, which ranges from 71.9 to 72.1 eV and is notably present only during and after cathodic polarization, consistent with a partial transformation to a Pt–H phase under HER conditions.[37]

The chemical composition of the Pt WE can be quantitatively compared as a function of applied potential by considering the ratio of the surface species to that of the Pt^0 metal (Figure 5). In comparison to the initial OCP (−200 mV), driving OER under alkaline conditions leads to a partially irreversible oxidation of Pt, increasing the amount of $Pt^{(II)}O$, Pt^{δ}–OH_{ads}, and the formation of $Pt^{(IV)}O_2$ on the surface, which persists upon returning to OCP after OER (−250 mV).[41]

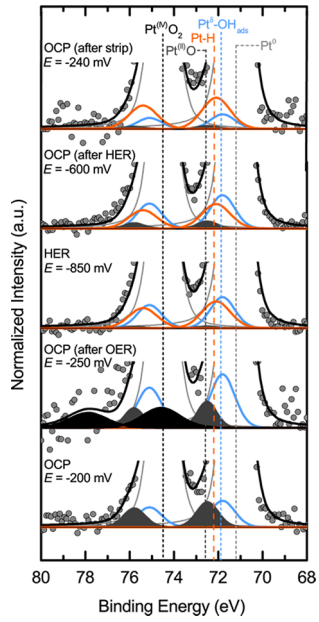

Figure 4. *Operando* APXPS Pt 4f photoelectron peak at 4 keV as a function of applied potential. Indicated is the position of the Pt^0 metal, Pt^{δ}–OH_{ads}, Pt–H, $Pt^{(II)}O$, and $Pt^{(IV)}O_2$ peaks. The scale is normalized to the background-subtracted intensity of the Pt^0 and magnified to highlight the changing surface species.

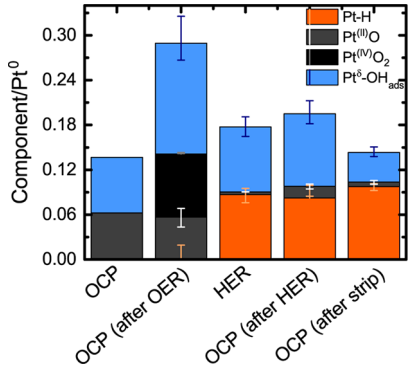

Figure 5. Stacked ratio of respective components in the Pt 4f relative to the Pt^0 metal peak as a function of applied potential. Error bars determined from Monte Carlo simulations (Supporting Information) are shown at the top of each component in corresponding hue (indicated as a line in the legend).

$Pt^{(II)}O$ and $Pt^{(IV)}O_2$ species are fully reduced under HER conditions (−850 mV), however, and the amount of Pt^{δ}–OH_{ads} decreases to an amount comparable to starting OCP conditions. Of note, we identify in *operando* an additional, oxygen-free species during HER at higher BE than Pt^0, likely arising from Pt–H species.[37]

Allowing the WE to relax following ~1 h of polarization under HER conditions results in a lower OCP (−600 mV), attributed in the literature to adsorbed H.[40] The surface chemistry remains largely unchanged under these conditions, consisting of both Pt^{δ}–OH_{ads} and Pt–H with comparable intensities. Anodic polarization is reported to "strip" adsorbed H and potentially adsorbed OH from the Pt surface, and following 10 cycles sweeping from −400 to +700 mV (Figure 1b, orange), the OCP returns to −240 mV. Stripping at such positive potentials leads to a notable decrease in the Pt^{δ}–OH_{ads}, consistent with adsorbed protonated species being stripped

DOI: 10.1021/acs.jpcb.7b06953
J. Phys. Chem. B 2018, 122, 864–870

from the surface. In contrast, the Pt−H component remains similar, suggesting that the Pt−H transformation and/or H intercalation persisted into the subsurface layer(s) during HER under alkaline conditions.

The presence of a feature >0.5 eV above the metal peak has been observed after H_2 exposure of Pt/MoO_3 composites.[37] The greater electronegativity of H compared to Pt can explain the formal oxidation of the metal during Pt−H formation. We note the formation of a potential hydride-like phase is suspected to be favorable only for small particle sizes;[36,37] however, the porous nature of Pt after electrochemical oxidation in alkaline solution[41] may impact the morphology during the present HER measurements which follow OER polarization, after the reduction of the $Pt^{(IV)}O_2$ overlayer and $Pt^{(II)}O$ species. Although the formation of a Pt-hydride phase is not frequently considered, its formation could have a dramatic impact on our understanding of the HER under alkaline conditions. In the case of Pd, well-known to form multiple hydride phases under cathodic polarization,[55] the too-strong adsorption (and subsequent absorption) of H limits HER activity.[56,57] While future experiments are needed to quantify the distribution of the potential hydride-like phase on Pt under alkaline conditions, its formation could be indicative of a H adsorption energy so strong under alkaline conditions that the formation of a near-surface hydride phase becomes energetically comparable, coming at a consequence to HER activity. The coexistence of Pt−H and $Pt^{\delta}-OH_{ads}$ may be promoted by the abstraction of H from water in alkaline environments,[58,59] and OH_{ads} species have been suggested to play a key role in strengthening the hydrogen adsorption energy under alkaline conditions.[28,60] Although we cannot make definitive claims regarding the reaction mechanism on Pt in alkaline environments, the accumulation of Pt−H in *operando* is consistent with the kinetics being determined by the discharge of H_{ads}.

CONCLUSIONS

This study brings new insight into the complexity of Pt surface speciation in *operando* during electrochemical polarization in alkaline environments. $Pt^{(II)}O$ and $Pt^{(IV)}O_2$ species formed during Pt oxidation and the OER, while exhibiting some hysteresis in their persistence at OCP following OER, are fully reduced at HER potentials and the subsequent OCP. In contrast, $Pt^{\delta}-OH_{ads}$ species are present under all conditions, potentially lending credence to the idea that OH_{ads} species can stabilize adsorbed H and impact the kinetics of HER under alkaline conditions. Furthermore, we observe an additional Pt species at higher BE during HER which does not correspond to any feature in the O 1s, indicative of adsorbed and absorbed H on or near the surface. Pt−H species persist after HER, and even following so-called "H-stripping" polarization to more anodic potentials, which instead decreases the amount of $Pt^{\delta}-OH_{ads}$. The complexity of the Pt speciation in *operando* suggests a unique reduction and oxidation behavior of $Pt^{\delta}-OH_{ads}$ and Pt−H in the subsurface layers during operation in alkaline electrolyte. This study highlights the need for *operando* techniques to develop new kinetic models for electrified interfaces under realistic operating conditions. Extending this experimental strategy to earth abundant materials will aid in the rational design of novel tailored materials for HER under alkaline conditions.

ASSOCIATED CONTENT

Supporting Information

The Supporting Information is available free of charge on the ACS Publications website at DOI: 10.1021/acs.jpcb.7b06953.

Error analysis, additional figures, and fitting parameters (PDF)

AUTHOR INFORMATION

Corresponding Authors

*E-mail: ejcrumlin@lbl.gov. Phone: +1-510-486-6235.
*E-mail: zhussain@lbl.gov. Phone: +1-510-486-7591.

ORCID

Kelsey A. Stoerzinger: 0000-0002-3431-8290
Marco Favaro: 0000-0002-3502-8332
Junko Yano: 0000-0001-6308-9071
Zhi Liu: 0000-0002-8973-6561
Zahid Hussain: 0000-0002-6434-5134
Ethan J. Crumlin: 0000-0003-3132-190X

Present Address

[&]M.F.: Helmholtz Zentrum Berlin für Materialien und Energie GmbH, Institute for Solar Fuels, Hahn-Meitner-Platz 1, D-14109 Berlin, Germany.

Author Contributions

[$]K.A.S., M.F.: These authors contributed equally.

Notes

The authors declare no competing financial interest.

ACKNOWLEDGMENTS

This work was partially supported through the Office of Science, Office of Basic Energy Science (BES), of the U.S. Department of Energy (DOE) under Award No. DE-SC0004993 to the Joint Center for Artificial Photosynthesis (JCAP), a DOE Energy Innovation Hub. The Advanced Light Source is supported by the Director, Office of Science, Office of Basic Energy Sciences, of the U.S. DOE under Contract No. DE-AC02-05CH11231. K.A.S. gratefully acknowledges support from the Linus Pauling Distinguished Post-Doctoral Fellowship Pacific Northwest National Laboratory (PNNL, Laboratory Directed Research and Development Program 69319). PNNL is a multiprogram national laboratory operated for DOE by Battelle.

REFERENCES

(1) Carrette, L.; Friedrich, K. A.; Stimming, U. Fuel Cells − Fundamentals and Applications. *Fuel Cells* **2001**, *1*, 5−39.
(2) Lewis, N. S.; Nocera, D. G. Powering the Planet: Chemical Challenges in Solar Energy Utilization. *Proc. Natl. Acad. Sci. U. S. A.* **2006**, *103*, 15729−15735.
(3) McKone, J. R.; Lewis, N. S.; Gray, H. B. Will Solar-Driven Water-Splitting Devices See the Light of Day? *Chem. Mater.* **2014**, *26*, 407−414.
(4) Stephens, I. E. L.; Rossmeisl, J.; Chorkendorff, I. Toward Sustainable Fuel Cells. *Science* **2016**, *354*, 1378−1379.
(5) Vesborg, P. C. K.; Seger, B.; Chorkendorff, I. Recent Development in Hydrogen Evolution Reaction Catalysts and Their Practical Implementation. *J. Phys. Chem. Lett.* **2015**, *6*, 951−957.
(6) Turner, J. A. Sustainable Hydrogen Production. *Science* **2004**, *305*, 972−974.
(7) Carpenter, B. K.; Harvey, J. N.; Orr-Ewing, A. J. The Study of Reactive Intermediates in Condensed Phases. *J. Am. Chem. Soc.* **2016**, *138*, 4695−4705.

DOI: 10.1021/acs.jpcb.7b06953
J. Phys. Chem. B 2018, 122, 864−870

(8) Crumlin, E. J.; Liu, Z.; Bluhm, H.; Yang, W.; Guo, J.; Hussain, Z. X-Ray Spectroscopy of Energy Materials under in Situ/Operando Conditions. *J. Electron Spectrosc. Relat. Phenom.* **2015**, *200*, 264−273.
(9) Kaya, S.; Ogasawara, H.; Näslund, L.-Å.; Forsell, J.-O.; Casalongue, H. S.; Miller, D. J.; Nilsson, A. Ambient-Pressure Photoelectron Spectroscopy for Heterogeneous Catalysis and Electrochemistry. Catal. *Catal. Today* **2013**, *205*, 101−105.
(10) Kornienko, N.; Resasco, J.; Becknell, N.; Jiang, C.-M.; Liu, Y.-S.; Nie, K.; Sun, X.; Guo, J.; Leone, S. R.; Yang, P. Operando Spectroscopic Analysis of an Amorphous Cobalt Sulfide Hydrogen Evolution Electrocatalyst. *J. Am. Chem. Soc.* **2015**, *137*, 7448−7455.
(11) Ramaker, D. E.; Korovina, A.; Croze, V.; Melke, J.; Roth, C. Following ORR Intermediates Adsorbed on a Pt Cathode Catalyst During Break-in of a PEM Fuel Cell by in Operando X-Ray Absorption Spectroscopy. *Phys. Chem. Chem. Phys.* **2014**, *16*, 13645−13653.
(12) Schlögl, R. Heterogeneous Catalysis. *Angew. Chem., Int. Ed.* **2015**, *54*, 3465−3520.
(13) Zandi, O.; Hamann, T. W. Determination of Photoelectrochemical Water Oxidation Intermediates on Haematite Electrode Surfaces Using Operando Infrared Spectroscopy. *Nat. Chem.* **2016**, *8*, 778−783.
(14) Vesborg, P. C. K.; Jaramillo, T. F. Addressing the Terawatt Challenge: Scalability in the Supply of Chemical Elements for Renewable Energy. *RSC Adv.* **2012**, *2*, 7933−7947.
(15) Fan, J.; Qi, K.; Zhang, L.; Zhang, H.; Yu, S.; Cui, X. Engineering Pt/Pd Interfacial Electronic Structures for Highly Efficient Hydrogen Evolution and Alcohol Oxidation. *ACS Appl. Mater. Interfaces* **2017**, *9*, 18008−18014.
(16) Kavian, R.; Choi, S.-I.; Park, J.; Liu, T.; Peng, H.-C.; Lu, N.; Wang, J.; Kim, M. J.; Xia, Y.; Lee, S. W. Pt-Ni Octahedral Nanocrystals as a Class of Highly Active Electrocatalysts toward the Hydrogen Evolution Reaction in an Alkaline Electrolyte. *J. Mater. Chem. A* **2016**, *4*, 12392−12397.
(17) Wang, P.; Zhang, X.; Zhang, J.; Wan, S.; Guo, S.; Lu, G.; Yao, J.; Huang, X. Precise Tuning in Platinum-Nickel/Nickel Sulfide Interface Nanowires for Synergistic Hydrogen Evolution Catalysis. *Nat. Commun.* **2017**, *8*, 14580.
(18) Conway, B. E.; Bockris, J. O. M. Electrolytic Hydrogen Evolution Kinetics and Its Relation to the Electronic and Adsorptive Properties of the Metal. *J. Chem. Phys.* **1957**, *26*, 532−541.
(19) Zeradjanin, A. R.; Grote, J.-P.; Polymeros, G.; Mayrhofer, K. J. J. A Critical Review on Hydrogen Evolution Electrocatalysis: Re-Exploring the Volcano-Relationship. *Electroanalysis* **2016**, *28*, 2256−2269.
(20) McCrory, C. C. L.; Jung, S.; Ferrer, I. M.; Chatman, S. M.; Peters, J. C.; Jaramillo, T. F. Benchmarking Hydrogen Evolving Reaction and Oxygen Evolving Reaction Electrocatalysts for Solar Water Splitting Devices. *J. Am. Chem. Soc.* **2015**, *137*, 4347−4357.
(21) Sheng, W.; Gasteiger, H. A.; Shao-Horn, Y. Hydrogen Oxidation and Evolution Reaction Kinetics on Platinum: Acid Vs Alkaline Electrolytes. *J. Electrochem. Soc.* **2010**, *157*, B1529−B1536.
(22) Cui, C.; Ahmadi, M.; Behafarid, F.; Gan, L.; Neumann, M.; Heggen, M.; Cuenya, B. R.; Strasser, P. Shape-Selected Bimetallic Nanoparticle Electrocatalysts: Evolution of Their Atomic-Scale Structure, Chemical Composition, and Electrochemical Reactivity under Various Chemical Environments. *Faraday Discuss.* **2013**, *162*, 91−112.
(23) Elbert, K.; Hu, J.; Ma, Z.; Zhang, Y.; Chen, G.; An, W.; Liu, P.; Isaacs, H. S.; Adzic, R. R.; Wang, J. X. Elucidating Hydrogen Oxidation/Evolution Kinetics in Base and Acid by Enhanced Activities at the Optimized Pt Shell Thickness on the Ru Core. *ACS Catal.* **2015**, *5*, 6764−6772.
(24) Rheinländer, P. J.; Herranz, J.; Durst, J.; Gasteiger, H. A. Kinetics of the Hydrogen Oxidation/Evolution Reaction on Polycrystalline Platinum in Alkaline Electrolyte Reaction Order with Respect to Hydrogen Pressure. *J. Electrochem. Soc.* **2014**, *161*, F1448−F1457.
(25) Sheng, W.; Myint, M.; Chen, J. G.; Yan, Y. Correlating the Hydrogen Evolution Reaction Activity in Alkaline Electrolytes with the Hydrogen Binding Energy on Monometallic Surfaces. *Energy Environ. Sci.* **2013**, *6*, 1509−1512.
(26) Sheng, W.; Zhuang, Z.; Gao, M.; Zheng, J.; Chen, J. G.; Yan, Y. Correlating Hydrogen Oxidation and Evolution Activity on Platinum at Different pH with Measured Hydrogen Binding Energy. *Nat. Commun.* **2015**, *6*, 5848.
(27) Zheng, J.; Sheng, W.; Zhuang, Z.; Xu, B.; Yan, Y. Universal Dependence of Hydrogen Oxidation and Evolution Reaction Activity of Platinum-Group Metals on pH and Hydrogen Binding Energy. *Sci. Adv.* **2016**, *2*, E1501602.
(28) Strmcnik, D.; Uchimura, M.; Wang, C.; Subbaraman, R.; Danilovic, N.; van der, V.; Paulikas, A. P.; Stamenkovic, V. R.; Markovic, N. M. Improving the Hydrogen Oxidation Reaction Rate by Promotion of Hydroxyl Adsorption. *Nat. Chem.* **2013**, *5*, 300−306.
(29) Ledezma-Yanez, I.; Wallace, W. D. Z.; Sebastián-Pascual, P.; Climent, V.; Feliu, J. M.; Koper, M. T. M. Interfacial Water Reorganization as a pH-Dependent Descriptor of the Hydrogen Evolution Rate on Platinum Electrodes. *Nature Energy* **2017**, *2*, 17031.
(30) Breiter, M. W. Electrochemical Study of Hydrogen Adsorption on Clean Platinum Metal Surfaces. *Ann. N. Y. Acad. Sci.* **1963**, *101*, 709−721.
(31) Gilroy, D.; Conway, B. E. Surface Oxidation and Reduction of Platinum Electrodes: Coverage, Kinetic and Hysteresis Studies. *Can. J. Chem.* **1968**, *46*, 875−890.
(32) Conway, B.; Bockris, J. Heats of Activation in Electrode Processes-the Electrochemical Desorption Mechanism of the Discharge of Hydronium Ions. *Can. J. Chem.* **1957**, *35*, 1124−1136.
(33) Conway, B. E.; Salomon, M. Isotope Effects in Electrochemical Proton Discharge. *Berichte der Bunsengesellschaft für physikalische Chemie* **1964**, *68*, 331−340.
(34) Will, F. G. Hydrogen Adsorption on Platinum Single Crystal Electrodes: I. Isotherms and Heats of Adsorption. *J. Electrochem. Soc.* **1965**, *112*, 451−455.
(35) BenDaniel, D. J.; Will, F. G. Effect of Hydrogen Absorbed by Electrode and Electrolyte on Hydrogen Coverage. *J. Electrochem. Soc.* **1967**, *114*, 909−915.
(36) Yamauchi, M.; Kobayashi, H.; Kitagawa, H. Hydrogen Storage Mediated by Pd and Pt Nanoparticles. *ChemPhysChem* **2009**, *10*, 2566−2576.
(37) Kalinkin, A. V.; Pashis, A. V.; Bukhtiyarov, V. I. X-Ray Photoelectron Study of the Interaction of H_2 and H_2+O_2 Mixtures on the Pt/MoO_3 Model Catalyst. *J. Struct. Chem.* **2008**, *49*, 255−260.
(38) Axnanda, S.; Crumlin, E. J.; Mao, B.; Rani, S.; Chang, R.; Karlsson, P. G.; Edwards, M. O. M.; Lundqvist, M.; Moberg, R.; Ross, P.; et al. Using "Tender" X-Ray Ambient Pressure X-Ray Photoelectron Spectroscopy as a Direct Probe of Solid-Liquid Interface. *Sci. Rep.* **2015**, *5*, 9788.
(39) Favaro, M.; Jeong, B.; Ross, P. N.; Yano, J.; Hussain, Z.; Liu, Z.; Crumlin, E. J. Unravelling the Electrochemical Double Layer by Direct Probing of the Solid/Liquid Interface. *Nat. Commun.* **2016**, *7*, 12695.
(40) Rodríguez-López, J.; Bard, A. J. Scanning Electrochemical Microscopy: Surface Interrogation of Adsorbed Hydrogen and the Open Circuit Catalytic Decomposition of Formic Acid at Platinum. *J. Am. Chem. Soc.* **2010**, *132*, 5121−5129.
(41) Favaro, M.; Valero-Vidal, C.; Eichhorn, J.; Toma, F. M.; Ross, P. N.; Yano, J.; Liu, Z.; Crumlin, E. J. Elucidating the Alkaline Oxygen Evolution Reaction Mechanism on Platinum. *J. Mater. Chem. A* **2017**, *5*, 11634−11643.
(42) Eilert, A.; Cavalca, F.; Roberts, F. S.; Osterwalder, J.; Liu, C.; Favaro, M.; Crumlin, E. J.; Ogasawara, H.; Friebel, D.; Pettersson, L. G. M.; et al. Subsurface Oxygen in Oxide-Derived Copper Electrocatalysts for Carbon Dioxide Reduction. *J. Phys. Chem. Lett.* **2017**, *8*, 285−290.
(43) Lichterman, M. F.; Hu, S.; Richter, M. H.; Crumlin, E. J.; Axnanda, S.; Favaro, M.; Drisdell, W.; Hussain, Z.; Mayer, T.; Brunschwig, B. S.; et al. Direct Observation of the Energetics at a

DOI: 10.1021/acs.jpcb.7b06953
J. Phys. Chem. B 2018, 122, 864−870

Semiconductor/Liquid Junction by Operando X-Ray Photoelectron Spectroscopy. *Energy Environ. Sci.* **2015**, *8*, 2409−2416.
(44) Hansen, W. N.; Kolb, D. M. The Work Function of Emersed Electrodes. *J. Electroanal. Chem. Interfacial Electrochem.* **1979**, *100*, 493−500.
(45) Daubinger, P.; Kieninger, J.; Unmussig, T.; Urban, G. A. Electrochemical Characteristics of Nanostructured Platinum Electrodes - a Cyclic Voltammetry Study. *Phys. Chem. Chem. Phys.* **2014**, *16*, 8392−8399.
(46) Reddy, A. K. N.; Genshaw, M. A.; Bockris, J. O. M. Ellipsometric Study of Oxygen-Containing Films on Platinum Anodes. *J. Chem. Phys.* **1968**, *48*, 671−675.
(47) Arrigo, R.; Hävecker, M.; Schuster, M. E.; Ranjan, C.; Stotz, E.; Knop-Gericke, A.; Schlögl, R. In Situ Study of the Gas-Phase Electrolysis of Water on Platinum by NAP-XPS. *Angew. Chem., Int. Ed.* **2013**, *52*, 11660−11664.
(48) van der Niet, M. J. T. C.; Garcia-Araez, N.; Hernández, J.; Feliu, J. M.; Koper, M. T. M. Water Dissociation on Well-Defined Platinum Surfaces: The Electrochemical Perspective. *Catal. Today* **2013**, *202*, 105−113.
(49) Binninger, T.; Fabbri, E.; Kötz, R.; Schmidt, T. J. Determination of the Electrochemically Active Surface Area of Metal-Oxide Supported Platinum Catalyst. *J. Electrochem. Soc.* **2014**, *161*, H121−H128.
(50) Law, Y. T.; Zafeiratos, S.; Neophytides, S. G.; Orfanidi, A.; Costa, D.; Dintzer, T.; Arrigo, R.; Knop-Gericke, A.; Schlogl, R.; Savinova, E. R. Situ Investigation of Dissociation and Migration Phenomena at the Pt/Electrolyte Interface of an Electrochemical Cell. *Chem. Sci.* **2015**, *6*, 5635−5642.
(51) Birss, V. I.; Damjanovic, A. Oxygen Evolution at Platinum Electrodes in Alkaline Solutions: I. Dependence on Solution pH and Oxide Film Thickness. *J. Electrochem. Soc.* **1987**, *134*, 113−117.
(52) Damjanovic, A.; Dey, A.; Bockris, J. O. M. Kinetics of Oxygen Evolution and Dissolution on Platinum Electrodes. *Electrochim. Acta* **1966**, *11*, 791−814.
(53) Wagner, F. T.; Moylan, T. E. A Comparison between Water Adsorbed on Rh(111) and Pt(111), with and without Predosed Oxygen. *Surf. Sci.* **1987**, *191*, 121−146.
(54) Saveleva, V. A.; Papaefthimiou, V.; Daletou, M. K.; Doh, W. H.; Ulhaq-Bouillet, C.; Diebold, M.; Zafeiratos, S.; Savinova, E. R. Operando near Ambient Pressure XPS (NAP-XPS) Study of the Pt Electrochemical Oxidation in H_2O and H_2O/O_2 Ambients. *J. Phys. Chem. C* **2016**, *120*, 15930−15940.
(55) Hu, C. C.; Wen, T. C. Effects of pH and Anion on Hydrogen Sorption/Desorption at/within Oxide-Derived Pd Electrodes. *J. Electrochem. Soc.* **1995**, *142*, 1376−1383.
(56) Quaino, P.; Santos, E. Hydrogen Evolution Reaction on Palladium Multilayers Deposited on Au(111): A Theoretical Approach. *Langmuir* **2015**, *31*, 858−867.
(57) Li, Y.; Chen, S.; Long, R.; Ju, H.; Wang, Z.; Yu, X.; Gao, F.; Cai, Z.; Wang, C.; Xu, Q.; et al. Near-Surface Dilution of Trace Pd Atoms to Facilitate Pd-H Bond Cleavage for Giant Enhancement of Electrocatalytic Hydrogen Evolution. *Nano Energy* **2017**, *34*, 306−312.
(58) Barber, J. H.; Conway, B. E. Structural Specificity of the Kinetics of the Hydrogen Evolution Reaction on the Low-Index Surfaces of Pt Single-Crystal Electrodes in 0.5 M Dm−3 NaOH. *J. Electroanal. Chem.* **1999**, *461*, 80−89.
(59) Schouten, K. J. P.; van der Niet, M. J. T. C.; Koper, M. T. M. Impedance Spectroscopy of H and OH Adsorption on Stepped Single-Crystal Platinum Electrodes in Alkaline and Acidic Media. *Phys. Chem. Chem. Phys.* **2010**, *12*, 15217−15224.
(60) Koper, M. T. M. Hydrogen Electrocatalysis: A Basic Solution. *Nat. Chem.* **2013**, *5*, 255−256.

DOI: 10.1021/acs.jpcb.7b06953
J. Phys. Chem. B 2018, 122, 864−870